ACS Photonics

Letter

pubs.acs.org/journal/apchd5

Light-Emission Enhancement in a Flexible and Size-Controllable ZnO Nanowire/Organic Light-Emitting Diode Array by the Piezotronic Effect

Rongrong Bao,[†,⊥] Chunfeng Wang,[†,‡,⊥] Zhengchun Peng,[§] Chuang Ma,[†,‡] Lin Dong,[†,‡] and Caofeng Pan*[,†]

[†]National Center for Nanoscience and Technology (NCNST), Beijing Institute of Nanoenergy and Nanosystems, Chinese Academy of Sciences, Beijing, 100083, China

[‡]The Key Laboratory of Materials Processing and Mold of Ministry of Education, School of Materials Science and Engineering, School of Physical Engineering, Zhengzhou University, Zhengzhou, 450001, China

[§]College of Optoelectronic Engineering, Shenzhen University, Shenzhen, 518060, China

Supporting Information

ABSTRACT: Enhancing the light emission of LED arrays by the piezotronic effect of ZnO NWs has recently attracted wide attention for the visual mapping of pressure. Here, to overcome deficiencies of ZnO LEDs, such as uncontrollable emission and poor emission efficiency, we designed a flexible, patterned ZnO/organic light-emitting device by combining the advantages of organic light-emitting materials and the piezoelectric effect of ZnO nanowires (NWs). The spatial resolution of the device can be tuned by the pattern size of the ZnO NW array. In addition, the light-emission character is solely determined by the organic light-emitting layer. The light-emission performance of the organic device is enhanced by the piezotronic transistors of the ZnO NW array through the modification of the energy band and reducing the Schottky barrier at the interface of the electrode and the semiconductor. By combining the advantages of the organic material and the piezotronic effect of ZnO NWs, this device shows potential for many applications, such as mechanosensation electronics.

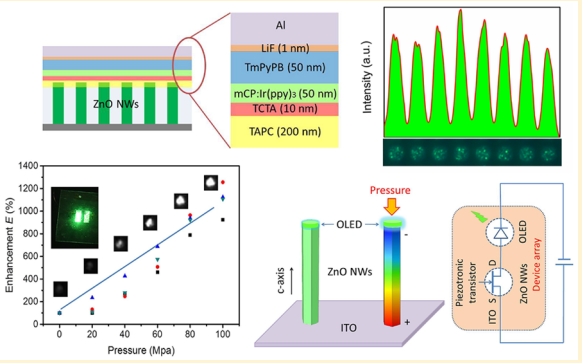

KEYWORDS: *wearable sensors, artificial skin, tactile sensing, pressure mapping, light-Emitting diode*

The creation of electronic skins, or tactile sensing devices, is a challenge for next-generation robotics and human–machine interfaces since the emulation of touching requires large-scale pressure sensor arrays with high spatial resolution, high sensitivity, and fast response.[1−5] Most electronic skin devices are based on resistance sensors or capacitive sensor arrays.[6−9] In these kinds of devices, the distribution of pressure is obtained by an electrical signal, and the pixels are read one at a time in serial acquisition.[10−12] A larger sensor with more pixels needs a longer time to record the pressure distribution data from the whole device surface. Therefore, this kind of device is suitable for static stress/pressure imaging instead of dynamic imaging, and it will not meet the requirements for application in electronic skins. By contrast, an optical signal can be used for parallel pressure distribution data recording, which is fast and has high enough efficiency to achieve high-resolution and dynamic stress measurement. Our group has reported relevant research about visual pressure distribution mapping by the piezo-phototronic effect of ZnO NW/GaN LED arrays.[13−15] Furthermore, we have reported a visual sensor based on ZnO/PEDOT:PSS LEDs[16−20] with the advantages of being flexible and fast and having high resolution in stress/pressure sensor applications, which has attracted much attention in recent years. However, in this kind of device structure, ZnO is not only the stress/pressure response material but also the n-type functional material and the emission layer. This leads to the emission of the LED array being associated with the defect emission of ZnO nanowires (NWs) grown by the low-temperature hydrothermal method. The uncontrollable emission color and poor emission efficiency of the device is inconvenient for the outputting and recording of the pressure distribution optical signal. In addition, this limits the application of this pressure sensor in electronic skins. Here, by combining the advantages of organic light-emitting devices[21−25] and the piezotronic effect of ZnO NWs,[26−31] we demonstrate a hybrid LED array based on ZnO NWs, which was used to fabricate a visual, flexible, high-resolution stress/pressure sensor. The spatial resolution of the light-emitting device array can be adjusted by the pattern size of the ZnO NW array, which can be controlled by the synthetic conditions, and the light-emission

Received: April 14, 2017
Published: May 18, 2017

DOI: 10.1021/acsphotonics.7b00386
ACS Photonics XXXX, XXX, XXX−XXX

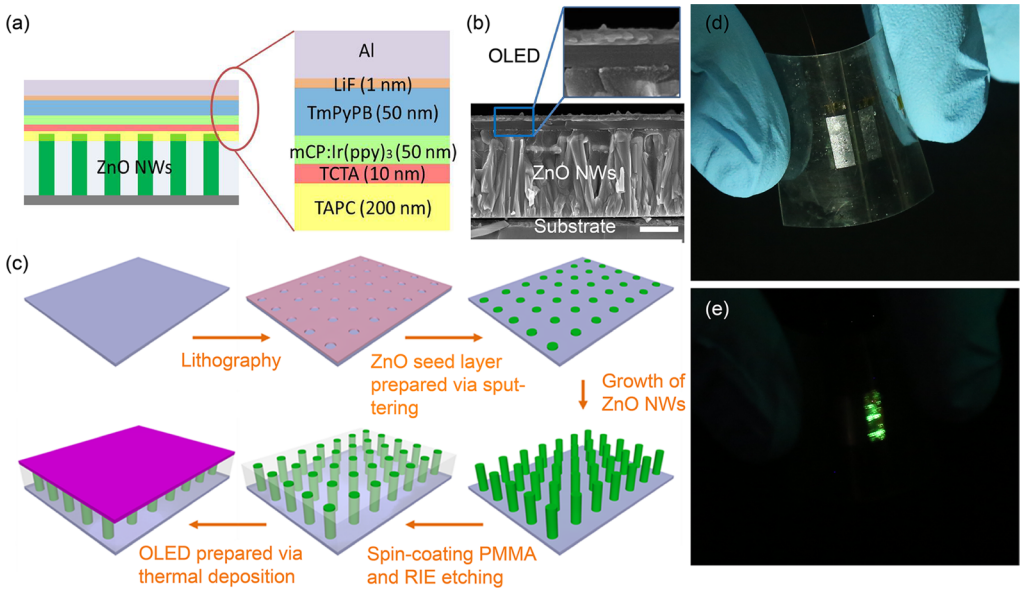

Figure 1. Schematic of the device structure and manufacturing process. (a) Schematic of the ZnO/organic LED. (b) SEM image of the device cross section (inset bar is 1 μm). (c) Manufacturing process of device fabrication. (d) Photograph of the flexible device and (e) the corresponding image when the device was lit.

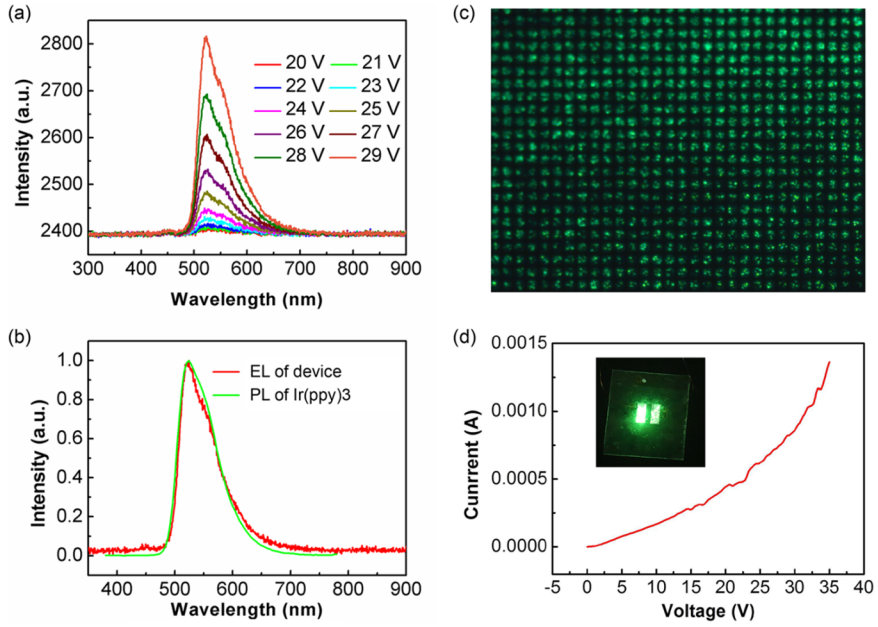

Figure 2. Characterization of the NW array LED. (a) EL spectra of the flexible NW/organic LED array under bias voltages ranging from 20 to 29 V. (b) Micrograph of the device that was electrically lit up at a bias voltage of 20 V, showing the green light emission from the NW array LED. (C) PL spectrum of $Ir(ppy)_3$ and the EL spectrum of the device. (d) $I-V$ curve of the device array. Inset is the optical image of device that was lit up.

performance is determined by the OLED layer. When the ZnO NW array is under applied pressure, the positive polarization charges caused by the piezotronic effect at the local interface between the ZnO NWs and the indium tin oxide (ITO) electrode modify the energy band and reduce the Schottky barrier at the interface of the electrode and the semiconductor, to increase the current in the device as the piezotronic transistors and thus enhance the light-emission intensity of the OLED. This flexible, ordered ZnO nanowire/organic LED array, fabricated on a poly(ethylene terephthalate) (PET) substrate, evidenced potential applications in the biomedical field and in artificial intelligence.

RESULTS AND DISCUSSION

As shown in Figure 1a, the structure of the device is divided into vertically grown ZnO NWs and the organic LED layer. Under pressure deformation, the ZnO NW layer controlled the current in the whole device as a piezotronic transistor. The luminescence properties of the device are determined entirely by the organic layer. The nanowire/organic LED device is based on a micropatterned array of ZnO NWs grown by the hydrothermal method on a prepatterned ITO/glass or ITO/PET (for flexible device fabrication) substrate (SEM images are shown in Figure S1). In addition, the *c*-axis of the ZnO NWs was pointed upward. Details of the growth of the NW array are

DOI: 10.1021/acsphotonics.7b00386
ACS Photonics XXXX, XXX, XXX−XXX

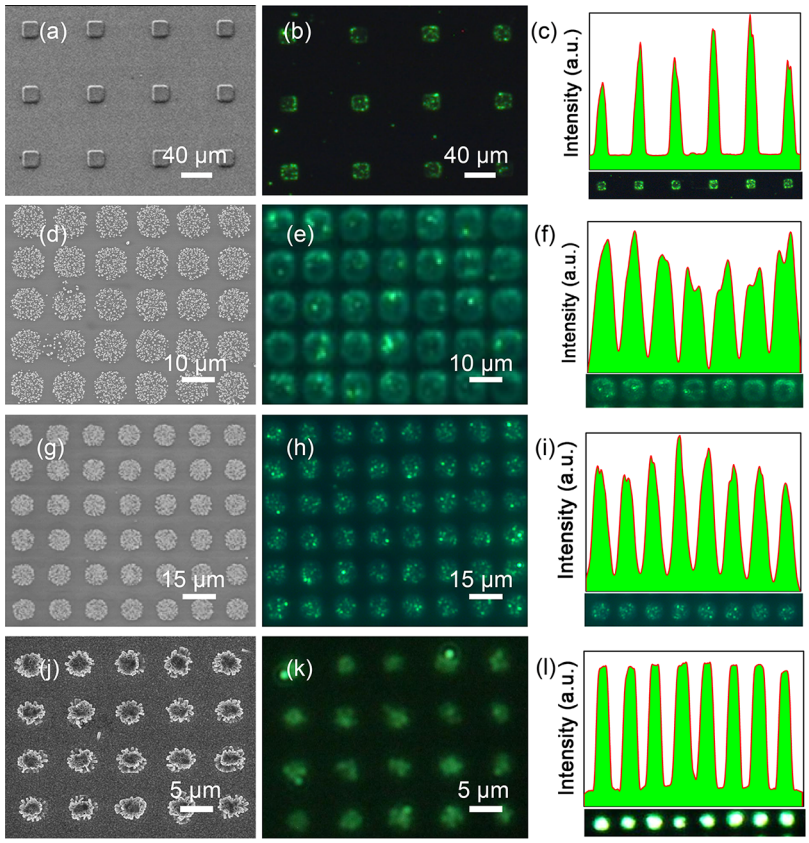

Figure 3. SEM images and optical microscopy images of the different sizes of light-emitting pixels in the array device and the corresponding line profiles of their emission intensity. (a), (b), and (c) have a side length of 20 μm and a pitch of 100 μm; (d), (e), and (f) have a side length of 10 μm and a pitch of 15 μm; (g), (h), and (i) have a side length of 5 μm and a pitch of 15 μm; and (j), (k), and (l) have a side length of 3 μm and a pitch of 8 μm.

shown in Figure S1, in which the size of the ZnO pattern has a side length of 10 μm and a pitch of 15 μm and the ZnO NWs have a diameter of 300 nm and a length of 3 μm. The interspaces of the nanowires were infiltrating with poly(methyl methacrylate) (PMMA), and then an organic layer was thermally evaporated on top. PMMA acts as a protecting layer for the nanowires and as insulation between the organic layer and the electrode on the substrate. The structure of the OLED is shown in Figure 1a. The devices consisted of the following structure from bottom to top: ITO-coated substrate/ZnO NW array/4,4′-cyclohexylidenebis[*N*,*N*-bis(*p*-tolyl)-aniline] (TAPC) hole transport layer (HTL) (200 nm)/tris(4-carbazoyl-9-ylphenyl)amine (TCTA) exciton blocking layer (EBL) (10 nm)/1,3-di-9-carbazolylbenzene (mCP):tris(2-phenylpyridinato-C^2,*N*)iridium(III) ($Ir(ppy)_3$) (6 wt %) emitting layer (EML) (50 nm)/1,3,5-tris(1-phenyl-1*H*-benzimidazol-2-yl)benzene (TPBi) electron transport layer (ETL) (50 nm)/LiF electron injection layer (EIL) (1 nm)/Al electrode (100 nm). Figure 1b shows a cross-sectional SEM image of the device. The inset in Figure 1b shows the layered structure of the OLED. It can be clearly seen that the device is divided into the ZnO NW layer, the organic layer, and the Al electrode layer. In general, ZnO NWs grow vertically, and the insulating polymer is filled between the nanowire gaps. The thickness of the organic layer is approximately 300 nm. Figure 1d shows a photograph of the flexible device. In addition, Figure 1e shows the corresponding image when the device was lit. We can clearly see the flexibility of the device and the bright green light emission as the device is bent.

The electroluminescence (EL) spectra of this flexible LED array device is shown in Figure 2a. We can see that the EL intensity of the LED array increases as the voltage increases. A visible emission ranging from 500 to 600 nm is observed as well, which is associated with the PL spectra of $Ir(ppy)_3$, as shown in Figure 2c. The PL of the ZnO NW array (shown in Figure S3) is composed of a near band edge (NBE) emission centered at 400 nm and a broad defect-related emission covering the range from 450 to 700 nm resulting from the hydrothermal synthesis process.[16,17] This clearly shows that the light emitted from the device was only from the organic material and not the ZnO NWs. A micrograph of the device was taken by electrically lighting up the device at a bias voltage of 25 V and is given in Figure 2b, showing green light emission from the NW array LED. The luminescence of the device is uniform over a large range. Figure 2d is the $I-V$ curve of the device array. The turn-on voltage of the device is approximately 20 V. The high turn-on voltage is due to the potential barrier in the device structure and the high resistance of the silver conductive adhesive connecting the Al electrode and the wire. The inset is the optical image of a device that was electrically lit up. It can be seen that the green emission intensity of the device is much clearer than that of the ZnO NW/PEDOT PSS device.[16]

The size of the light-emitting pixels is defined by the ZnO NW array. We fabricated different sizes of ZnO NW arrays by lithography to fabricate the light-emitting device. The size of the light-emitting pixels can be adjusted from 20 μm to 3 μm and the pitch from 100 μm to 8 μm. As shown in Figure 3,

DOI: 10.1021/acsphotonics.7b00386
ACS Photonics XXXX, XXX, XXX−XXX

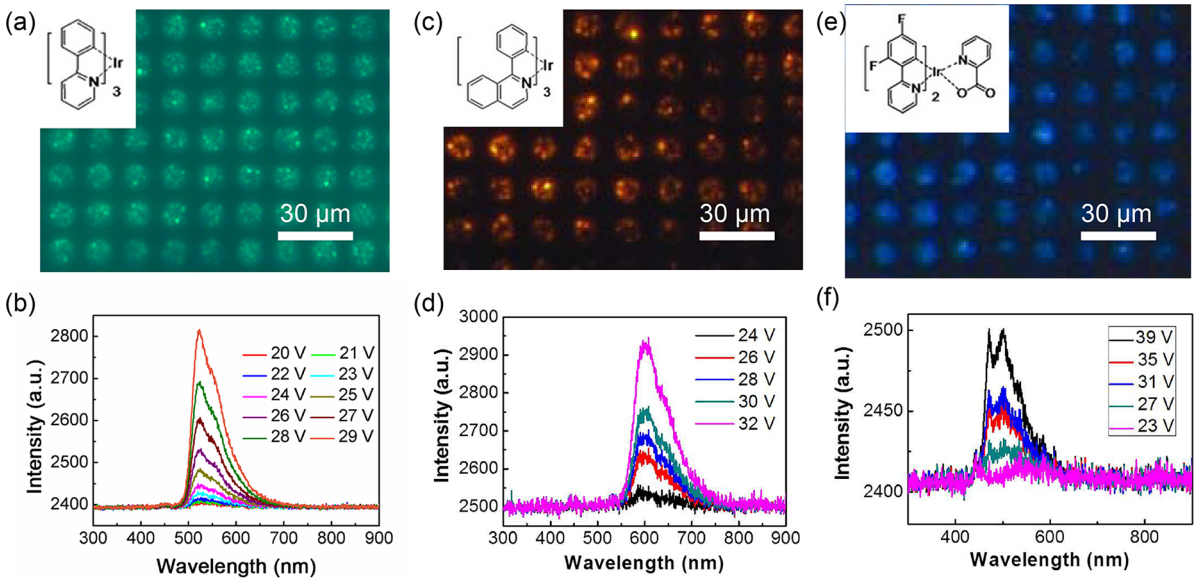

Figure 4. Micrographs and EL spectra of array devices with different colors. The inset pictures show the molecular structure of the fluorescent molecules.

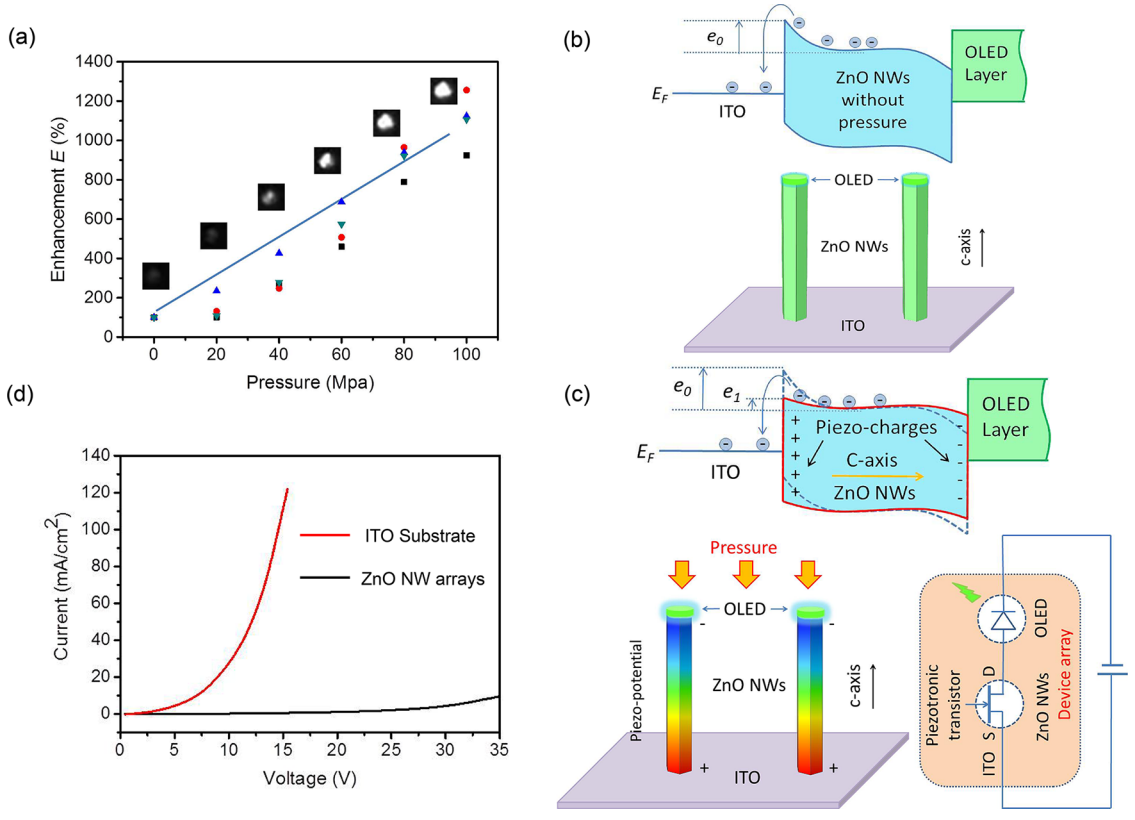

Figure 5. (a) Enhancement factor E of the light-emission performance of NW LEDs under different applied pressures of up to 100 MPa. (b) Schematic band diagram of a ZnO/organic LED NW without applying a compressive strain. The Schottky barrier in the interface between ITO and the ZnO NW limits the current in the device. (c) Schematic band diagram of a ZnO under (solid line) applying a compressive strain. Upon applying pressure, a positive piezopotential is induced at the Schottky contact, which reduces the barrier height at that contact and hence increases the transport conductance of the ZnO NWs. The inset is a schematic of the device equivalent circuit. The ZnO NW plays a role of piezotronic transistor. Piezopotential distributions occur in a ZnO nanowire under applied pressure and thus enhance the current and light emission intensity of the device. (d) Current density−voltage characteristics of the devices with ZnO NWs and without NWs.

comparing the SEM images of the ZnO NW arrays and the microscope images of the lit-up device fabricated by the same ZnO NW arrays, the device emission coincides with the position of the ZnO NWs. The corresponding line profiles of the emission intensity of several typical nanowire LEDs show that the light emission is uniform, and no crosstalk between adjacent light-emitting pixels is observed. This is important in applications in sensor arrays, in which the range of pressure and

DOI: 10.1021/acsphotonics.7b00386
ACS Photonics XXXX, XXX, XXX−XXX

mapping resolution are defined by the size of the emission pixels.

In this kind of device, the ZnO NW layer is the sole stress-response layer that changes the energy band through polarization charges, and the light-emission properties are determined solely by the organic layer. The multicolor and multitudinous character of the organic material gives our device the advantages of multifunction and more options to meet the needs of different requirements. The light emission of the device can be tuned by doping an organic phosphorescent material in the light-emitting layer. When we change $Ir(ppy)_3$ to $Ir(piq)_3$ (tris(1-phenylisoquinolinato-C^2,N)iridium(III)) or FIrPic (bis[2-(4,6-difluorophenyl)pyridinato-C^2,N]-(picolinato)iridium(III)), the light emission color of the device changes to red and blue. Micrographs of different color devices lit up and room-temperature EL spectra are shown in Figure 4. Doping with two or three fluorescent molecules can produce a variety of colors to meet different application needs.

A measurement system based on an inverted microscope and 3D micromanipulation stages was used to measure the piezotronic effect of the ZnO NWs on the device performance of the LED array with respect to light emission. As shown in Figure 5a, the enhancement factor E (E is the ratio between the luminous intensity upon compression and the original luminous intensity) of the NW LEDs with applied compressive pressures up to 100 MPa clearly shows that a greater applied pressure leads to a higher illumination intensity. The light emission from the device under different pressures is shown in Figure S4. Changes in light emission in the array LED device are present only in the area compressed by the stamp (patterned as the letter "C"). The obvious enhancement in light emission of the NW array LED under different pressures is due to the piezotronic effect from the ZnO NW array. Figure 5b and c show the energy band diagram and the simulated piezopotential distributions in the ZnO NW array before (b) and after (c) applying pressure. According to the equivalent circuit of the device, ZnO NWs play the role of piezotronic transistor connected with an OLED in series and adjusting the current in the circuit by the piezopotential distributions in a ZnO nanowire under applied pressure. As shown from the current density−voltage characteristics in Figure 5d, the threshold turn-on voltage is 10 V or less for the OLED device without the ZnO NW array (the device structure is shown in Figure S5), while the threshold voltage of the device based on the NW array is increased to more than 20 V. Meanwhile, the current density of the device based on the ZnO NW array is also much less than the device on the ITO substrate, which is due to the Schottky barrier at the interface between ZnO NWs and ITO to reduce the current in the device and the voltage on the OLED layer. When ZnO NWs are under the compressive stress, the positive polarization charges caused by the piezotronic effect at the local interface between the ZnO NWs and the ITO electrode will modify the energy band at the interface of the electrode and the semiconductor to reduce the Schottky barrier and thus decrease the resistivity of the ZnO NWs. Therefore, the current in the whole device and the light-emission intensity of the OLED will be enhanced.[20,26] The pressure range of this device is about 0∼100MPa. When the pressure is increased beyond the maximum range of that the device can withstand, the most easily damaged part of this device is the layer of organic layer (about 350 nm). When the device withstands high pressure, the layer of organic layer will be first damage and lead to short circuits.[16] Additional photographs of the flexible device are shown in Figure S6. This ZnO/organic LED device is flexible and stable. After repeated bending, it maintains its luminous intensity, even after normal light is cut in half.

CONCLUSIONS

In summary, we demonstrated a NW/organic LED array based on a ZnO NW array grow on a flexible substrate, where the spatial resolution of the array device, the emitting pixels, can be controlled by the growth conditions of the ZnO NW array. Light emission from the device solely comes from the organic layer and can be tuned by doping with fluorescent molecules. Meanwhile, the device performance with respect to the luminous intensity was enhanced by strain-induced piezoelectric polarization charges at the interface of the ZnO NWs and the organic layer, which increased the rate of hole injection during the emission process. Combing the advantages of the organic material and the piezotronic effect of the ZnO NW array, this device will find applications in many fields, such as electronic skins, biomedical science, and security technology.

EXPERIMENTAL SECTION

Fabrication of the Device. First, the substrates were ultrasonically cleaned with acetone, isopropyl alcohol, and deionized water for 10 min, and then the preprepared patterns with different pore diameters and pitches were applied by photolithography. The ZnO NW array was prepared on the patterned substrate by the hydrothermal method previously reported. The interspaces of the nanowires were infiltrated with PMMA as a protecting layer for the nanowires and as insulation between the organic layer and the electrode. Finally, a layer of OLED material was deposited by thermal evaporation. Organic materials were purchased from Xi'an Polymer Light Technology Corp. (>99%, HPLC) and sublimed without further purification.

Characterization. Optical images of the LED arrays were measured using a Zeiss Observer inverted microscope. The EL spectra were collected on an Ocean Optics QE65000 spectrometer. The piezotronic effect measurement system was made of the inverted microscope and a 3D micromanipulation stage with a dynamometer. The output light intensity was recorded by an HQ2 camera, and the enhancement in light emission was analyzed through image acquisition and processing technologies.

ASSOCIATED CONTENT

Supporting Information

The Supporting Information is available free of charge on the ACS Publications website at DOI: 10.1021/acsphotonics.7b00386.

Figures S1−S6 show further details of the ZnO arrays and the device performance (PDF)

AUTHOR INFORMATION

Corresponding Author

*E-mail (C. Pan): cfpan@binn.cas.cn.

ORCID

Lin Dong: 0000-0002-4126-6812

Caofeng Pan: 0000-0001-7693-5388

Author Contributions

⊥R. Bao and C. Wang contributed equally to this work.

DOI: 10.1021/acsphotonics.7b00386
ACS Photonics XXXX, XXX, XXX−XXX

Notes

The authors declare no competing financial interest.

■ ACKNOWLEDGMENTS

The authors are thankful for the support from the National Natural Science Foundation of China (Nos. 61505010, 61675027, 61405040, 51622205, and 51432005), the support of the National Key R & D Project from the Minister of Science and Technology, China (2016YFA0202703), and the "Thousand Talents" Program of China for pioneering researchers and innovative teams.

■ REFERENCES

(1) Wang, X.; Dong, L.; Zhang, H.; Yu, R.; Pan, C.; Wang, Z. L. Recent progress in electronic skin. *Advanced Science* **2015**, *2* (10).150016910.1002/advs.201500169

(2) Chortos, A.; Bao, Z. N. Skin-inspired electronic devices. *Mater. Today* **2014**, *17* (7), 321−331.

(3) Hammock, M. L.; Chortos, A.; Tee, B. C. K.; Tok, J. B. H.; Bao, Z. A. 25th Anniversary Article: The Evolution of Electronic Skin (E-Skin): A Brief History, Design Considerations, and Recent Progress. *Adv. Mater.* **2013**, *25* (42), 5997−6037.

(4) Bauer, S. Flexible Electronics Sophisticated skin. *Nat. Mater.* **2013**, *12* (10), 871−872.

(5) Wang, X. D.; Zhang, H. L.; Yu, R. M.; Dong, L.; Peng, D. F.; Zhang, A. H.; Zhang, Y.; Liu, H.; Pan, C. F.; Wang, Z. L. Dynamic Pressure Mapping of Personalized Handwriting by a Flexible Sensor Matrix Based on the Mechanoluminescence Process. *Adv. Mater.* **2015**, *27* (14), 2324−2331.

(6) Zhao, X.; Hua, Q.; Yu, R.; Zhang, Y.; Pan, C. Flexible, stretchable and wearable multifunctional sensor array as artificial electronic skin for static and dynamic strain mapping. *Advanced Electronic Materials* **2015**, *1* (7), 1500142.

(7) Hua, Q.; Liu, H.; Zhao, J.; Peng, D.; Yang, X.; Gu, L.; Pan, C. Bioinspired Electronic Whisker Arrays by Pencil-Drawn Paper for Adaptive Tactile Sensing. *Advanced Electronic Materials* **2016**, *2* (5), 1600093.

(8) Wang, Y.; Wang, L.; Yang, T. T.; Li, X.; Zang, X. B.; Zhu, M.; Wang, K. L.; Wu, D. H.; Zhu, H. W. Wearable and Highly Sensitive Graphene Strain Sensors for Human Motion Monitoring. *Adv. Funct. Mater.* **2014**, *24* (29), 4666−4670.

(9) Tee, B. C. K.; Chortos, A.; Dunn, R. R.; Schwartz, G.; Eason, E.; Bao, Z. A. Tunable Flexible Pressure Sensors using Microstructured Elastomer Geometries for Intuitive Electronics. *Adv. Funct. Mater.* **2014**, *24* (34), 5427−5434.

(10) Chen, M.; Li, X.; Lin, L.; Du, W.; Han, X.; Zhu, J.; Pan, C.; Wang, Z. L. Triboelectric Nanogenerators as a Self-Powered Motion Tracking System. *Adv. Funct. Mater.* **2014**, *24* (32), 5059−5066.

(11) Wang, X.; Zhang, H.; Dong, L.; Han, X.; Du, W.; Zhai, J.; Pan, C.; Wang, Z. L. Self-Powered High-Resolution and Pressure-Sensitive Triboelectric Sensor Matrix for Real-Time Tactile Mapping. *Adv. Mater.* **2016**, *28* (15), 2896−2903.

(12) Mannsfeld, S. C. B.; Tee, B. C. K.; Stoltenberg, R. M.; Chen, C. V. H. H.; Barman, S.; Muir, B. V. O.; Sokolov, A. N.; Reese, C.; Bao, Z. Highly sensitive flexible pressure sensors with microstructured rubber dielectric layers. *Nat. Mater.* **2010**, *9* (10), 859−864.

(13) Chen, M.; Pan, C.; Zhang, T.; Li, X.; Liang, R.; Wang, Z. Tuning Light Emission of a Pressure Sensitive Silicon/ZnO Nanowires Heterostructure Matrix Through Piezo-Phototronic Effect. *ACS Nano* **2016**, *10* (6), 6074−6079.

(14) Li, X. Y.; Chen, M. X.; Yu, R. M.; Zhang, T. P.; Song, D. S.; Liang, R. R.; Zhang, Q. L.; Cheng, S. B.; Dong, L.; Pan, A. L.; Wang, Z. L.; Zhu, J.; Pan, C. F. Enhancing Light Emission of ZnO-Nanofilm/Si-Micropillar Heterostructure Arrays by Piezo-Phototronic Effect. *Adv. Mater.* **2015**, *27* (30), 4447−4453.

(15) Pan, C. F.; Dong, L.; Zhu, G.; Niu, S. M.; Yu, R. M.; Yang, Q.; Liu, Y.; Wang, Z. L. High-resolution electroluminescent imaging of pressure distribution using a piezoelectric nanowire LED array. *Nat. Photonics* **2013**, *7* (9), 752−758.

(16) Bao, R. R.; Wang, C. F.; Dong, L.; Yu, R. M.; Zhao, K.; Wang, Z. L.; Pan, C. F. Flexible and Controllable Piezo-Phototronic Pressure Mapping Sensor Matrix by ZnO NW/p-Polymer LED Array. *Adv. Funct. Mater.* **2015**, *25* (19), 2884−2891.

(17) Wang, C. F.; Ba, R. R.; Zhao, K.; Zhang, T. P.; Dong, L.; Pan, C. F. Enhanced emission intensity of vertical aligned flexible ZnO nanowire/p-polymer hybridized LED array by piezo-phototronic effect. *Nano Energy* **2015**, *14*, 364−371.

(18) Pan, C.; Dong, L.; Zhu, G.; Niu, S.; Yu, R.; Yang, Q.; Liu, Y.; Wang, Z. L. High-resolution electroluminescent imaging of pressure distribution using a piezoelectric nanowire LED array. *Nat. Photonics* **2013**, *7* (9), 752−758.

(19) Bao, R.; Wang, C.; Dong, L.; Shen, C.; Zhao, K.; Pan, C. CdS nanorods/organic hybrid LED array and the piezo-phototronic effect of the device for pressure mapping. *Nanoscale* **2016**, *8* (15), 8078−8082.

(20) Wu, W. Z.; Wen, X. N.; Wang, Z. L. Taxel-Addressable Matrix of Vertical-Nanowire Piezotronic Transistors for Active and Adaptive Tactile Imaging. *Science* **2013**, *340* (6135), 952−957.

(21) Faria, J. C. D.; Campbell, A. J.; McLachlan, M. A. ZnO Nanorod Arrays as Electron Injection Layers for Efficient Organic Light Emitting Diodes. *Adv. Funct. Mater.* **2015**, *25* (29), 4657−4663.

(22) Hofle, S.; Bruns, M.; Strassle, S.; Feldmann, C.; Lemmer, U.; Colsmann, A. Tungsten Oxide Buffer Layers Fabricated in an Inert Sol-Gel Process at Room-Temperature for Blue Organic Light-Emitting Diodes. *Adv. Mater.* **2013**, *25* (30), 4113−4116.

(23) Chiba, T.; Pu, Y. J.; Miyazaki, R.; Nakayama, K.; Sasabe, H.; Kido, J. Ultra-high efficiency by multiple emission from stacked organic light-emitting devices. *Org. Electron.* **2011**, *12* (4), 710−715.

(24) Dias, F. B.; Bourdakos, K. N.; Jankus, V.; Moss, K. C.; Kamtekar, K. T.; Bhalla, V.; Santos, J.; Bryce, M. R.; Monkman, A. P. Triplet Harvesting with 100% Efficiency by Way of Thermally Activated Delayed Fluorescence in Charge Transfer OLED Emitters. *Adv. Mater.* **2013**, *25* (27), 3707−3714.

(25) Nakayama, Y.; Morii, K.; Suzuki, Y.; Machida, H.; Kera, S.; Ueno, N.; Kitagawa, H.; Noguchi, Y.; Ishii, H. Origins of Improved Hole-injection Efficiency by the Deposition of MoO3 on the Polymeric Semiconductor Poly (dioctylfluorene-alt-benzothiadiazole). *Adv. Funct. Mater.* **2009**, *19* (23), 3746−3752.

(26) Wang, Z. L. Piezopotential gated nanowire devices: Piezotronics and piezo-phototronics. *Nano Today* **2010**, *5* (6), 540−552.

(27) Yu, R. M.; Wang, X. F.; Wu, W. Z.; Pan, C. F.; Bando, Y.; Fukata, N.; Hu, Y. F.; Peng, W. B.; Ding, Y.; Wang, Z. L. Temperature Dependence of the Piezo-phototronic Effect in CdS Nanowires. *Adv. Funct. Mater.* **2015**, *25* (33), 5277−5284.

(28) Zhang, F.; Niu, S. M.; Guo, W. X.; Zhu, G.; Liu, Y.; Zhang, X. L.; Wang, Z. L. Piezo-phototronic Effect Enhanced Visible/UV Photodetector of a Carbon-Fiber/ZnO-CdS Double-Shell Microwire. *ACS Nano* **2013**, *7* (5), 4537−4544.

(29) Yang, Q.; Liu, Y.; Pan, C.; Chen, J.; Wen, X.; Wang, Z. L. Largely Enhanced Efficiency in ZnO Nanowire/p-Polymer Hybridized Inorganic/Organic Ultraviolet Light-Emitting Diode by Piezo-Phototronic Effect. *Nano Lett.* **2013**, *13* (2), 607−613.

(30) Wang, Z. L. Progress in Piezotronics and Piezo-Phototronics. *Adv. Mater.* **2012**, *24* (34), 4632−4646.

(31) Wang, Z. L.; Yang, R. S.; Zhou, J.; Qin, Y.; Xu, C.; Hu, Y. F.; Xu, S. Lateral nanowire/nanobelt based nanogenerators, piezotronics and piezo-phototronics. *Mater. Sci. Eng., R* **2010**, *70* (3−6), 320−329.

DOI: 10.1021/acsphotonics.7b00386
ACS Photonics XXXX, XXX, XXX−XXX